Journal of Zhejiang University SCIENCE A
ISSN 1673-565X (Print); ISSN 1862-1775 (Online)
www.zju.edu.cn/jzus; www.springerlink.com
E-mail: jzus@zju.edu.cn

Investigation on the automatic parameters extraction of pulse signals based on wavelet transform

WANG Hui-yan[1], ZHANG Pei-yong[†‡2]

([1]*College of Computer Science & Information Engineering, Zhejiang Gongshang University, Hangzhou 310018, China*)

([2]*Institute of VLSI Design, Zhejiang University, Hangzhou 310027, China*)

[†]E-mail: zhangpy@vlsi.zju.edu.cn

Received Mar. 1, 2007; revision accepted Apr. 28, 2007

Abstract: This paper analyses a key problem in the quantification of pulse diagnosis. Due to the subjectivity and fuzziness of pulse diagnosis, quantitative methods are needed. To extract the parameters of pulse signals, the prerequisite is to detect the corners of pulse signals correctly. Up to now, the pulse parameters are mostly acquired by marking the pulse corners manually, which is an obstacle to modernize pulse diagnosis. Therefore, a new automatic parameters extraction approach for pulse signals using wavelet transform is presented. The results testified that the method we proposed is feasible and effective and can detect corners of pulse signals accurately, which can be expected to facilitate the modernization of pulse diagnosis.

Key words: Pulse signal, Feature extraction, Complex wavelet transform, Quantitative diagnosis
doi:10.1631/jzus.2007.A1283 **Document code:** A **CLC number:** TP391

INTRODUCTION

Pulse diagnosis is one of the most important examinations. Doctors diagnose the patient by feeling the pulse beating at the measuring point of the radial artery, which requires long experiences and a high level of skill. Traditional pulse diagnosis is subjective and deficient in quantitative criteria of diagnosis. Therefore, quantitative methods are needed. Although much effort is being spent on pulse analysis (Lee *et al.*, 1993; Yoon *et al.*, 2000; Wang and Cheng, 2005; Xu *et al.*, 2006; Xu and Zhang, 2007), there is still no efficient and effective method of automatic pulse parameters computation. In the pioneering works, pulse signal corners were mostly marked manually and the parameters were extracted by ocular estimation, which undoubtedly impeded the modernization of pulse classification and its applications in clinic.

Pulse signal is a kind of weak, nonstationary, low-frequency signal and can be easily contaminated by background noises, such as the uncontrollable movements of body limbs. The pulse parameters are computed based on the corners of pulse signals (Fei, 2003). So the first step is to detect the corners of pulse signals. An attractive tool for analyzing the local behavior of such signals is wavelet transform (WT), which can decompose signals into elementary building blocks that are well localized both in space and frequency (Mallat and Zhong, 1992). Corners are locations where the curvature changes sharply and are regarded as the most descriptive features and can be characterized by the modulus of their WTs (Lee *et al.*, 1995). Recently, several corner detection techniques based on WT (Lee *et al.*, 1995; Quddus and Fahmy, 1999; Sun *et al.*, 2004) have been proposed and applied in some domains, such as object recognition (Sun *et al.*, 2004). In traditional corner detection methods based on WT, the scale s and modulus threshold t need to be determined by the trial-and-error method, which is often deficient and time-

‡ Corresponding author

consuming. In order to detect the characteristic points of pulse signals effectively, a new pulse parameter extraction approach is proposed and tested in this work.

CHARACTERISTICS OF PULSE SIGNAL

Generally, pulse signals are classified according to seven factors: depth, width, length, frequency, rhythm and strength. Fig.1 is an example of pulse signal obtained through a pulse transducer. As the contact pressure of pulse transducer increases, the amplitude of the pulse signal first increases, reaching a maximum point, and then decreases. Therefore, one period of pulse signal is composed of three parts: *SP*, *EF* and *FG* (Fig.1). The main pulse parameters (Fei, 2003) that need to be detected are marked by the dashed lines in Fig.1, where P', E', F', G', K' and L' are the projections of *P*, *E*, *F*, *G*, *K* and *L* onto the *x* axis, respectively. These parameters are listed as follows: P_1 represents the optimal contact pressure, under which the maximum amplitude of pulse signal is attained; h_{sp} represents the height of *SP*, shown as PP'; h_{ef} represents the height of *EF*, shown as KK'; h_{fg} represents the height of *FG*, shown as LL'; h_{ff} represents the height of the starting point of *FG*, shown as FF'; h_{ee} represents the height of the starting point of *EF*, shown as EE'; C_1 represents the periodicity of the pulse signal; A_1 represents the dimension of the pulse signal in one cycle.

These parameters are meaningful in medicine (Fei, 2003; Wang and Cheng, 2005) and testified to be effective in pulse analysis. Other characteristics can be computed through these parameters. Fig.1 shows

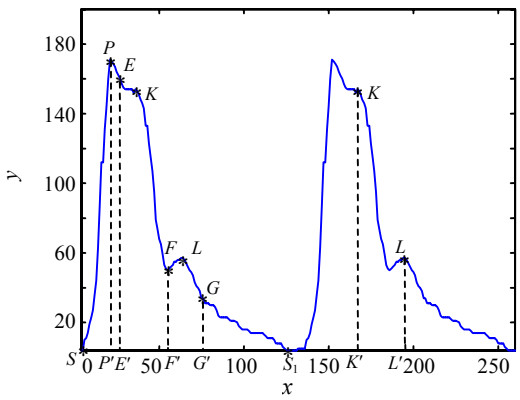

Fig.1 Characteristic parameters of the pulse signal

that the characteristic parameters are computed based on the seven corners of pulse signal, marked as *S*, *P*, *E*, *K*, *L*, *G* and S_1, respectively.

NOISE REDUCTION OF PULSE SIGNAL

To reduce the disturbance of background noise in pulse signals, we use the wavelet decomposition-reconstruction algorithm. For the original pulse signal $f_r(x)$, wavelet decomposition coefficients are given by

$$\begin{cases} c_k^{(j)} = \sum_n h_0(n-2k)x_n^{(j+1)}, \\ d_k^{(j)} = \sum_n h_1(n-2k)x_n^{(j+1)}, \end{cases} \tag{1}$$

where $h_0(n)$ and $h_1(n)$ represent a pair of filter banks; $c_k^{(j)}$ and $d_k^{(j)}$ represent the coarse coefficients and detail coefficients in resolution *j*, respectively.

On the other hand, with these multiscale representations, the original signal $f(x)$ can be reconstructed through

$$x_n^{(j+1)} = \sum_k h_0(n-2k)c_k^{(j)} + \sum_k h_1(n-2k)d_k^{(j)}. \tag{2}$$

The pulse signal $f(x)$ corresponds to the low frequency of the non-stationary signal $f_r(x)$ and represents the main outline of signal; the background noise corresponds to the high frequency and represents the detail. Therefore, the wavelet decomposition coefficients of the background noise mainly concentrate on $d_k^{(j)}$. Based on this fact, the algorithm of noise reduction can be described step by step as follows:

Step 1: Select one wavelet function $\psi(x)$ and decide the wavelet decomposition layer *J*.

Step 2: Decompose the pulse signal $f_r(x)$ by wavelet $\psi(x)$ in each layer according to Eq.(1) and get the wavelet coefficient c_j and d_j, where j=1,2,..,*J*.

Step 3: Decide the optimum scale α, assign null to detail coefficient d_α and reconstruct the pulse signal $f(x)$ from the coarse coefficient c_α according to Eq.(2).

Step 4: Set threshold value *T* and compute sig-

nal-to-noise ratio κ. When $\kappa<T$, select another wavelet function $\psi(x)$ and repeat Step 2 and Step 3. When $\kappa>T$, the signal $f(x)$ is taken as a net signal and used for the subsequent processing.

The selection of wavelet function and the decision of wavelet decomposition layer is the key in the algorithm. By simulation, we found that smooth and symmetric wavelet function, such as Mexican Hat wavelet, can reduce noise effectively and preserve the important information of the pulse signal at the same time. In addition, we found that the optimum scale α is 4.

PARAMETER EXTRACTION

Let $\psi(x)$ be a complex-valued wavelet, the continuous wavelet transform of the pulse signal $f(x)$ with respect to the wavelet $\psi(x)$ is defined as

$$Wf(a,b)=\int_{-\infty}^{+\infty} f(x)\overline{\psi}_a(x-b)\mathrm{d}x, \tag{3}$$

where $\psi_\alpha(x)=[\alpha\psi(x/\alpha)]^{-1}$ and $\overline{\psi}_a(x)$ denotes the complex conjugate of $\psi_\alpha(x)$.

We choose the second derivative of the Gaussian function $\theta_\delta(x)$, which has two vanishing moments (Mallat and Hwang, 1992), as the real-valued wavelet $\psi^{\mathrm{r}}(x)$:

$$\psi_\sigma^{\mathrm{r}}(x)=-\frac{\mathrm{d}^2\theta_\delta(x)}{\mathrm{d}x^2}. \tag{4}$$

The modulus maxima of the wavelet transform correspond to the curvature of high order. Then the real wavelet transform of $f(x)$ is written as

$$Wf^{\mathrm{r}}=f(x)*\psi_\sigma^{\mathrm{r}}(x)=\sigma^2 f(x)*\frac{\mathrm{d}^2\theta_\delta(x)}{\mathrm{d}x^2}. \tag{5}$$

We turn the real-valued wavelet $\psi^{\mathrm{r}}(x)$ into complex-valued wavelet by means of Hilbert transform H (Tu and Hwang, 2005):

$$\psi(x)=(1+\mathrm{j}H)\psi_\sigma^{\mathrm{r}}(x). \tag{6}$$

The frequency response of $\psi(x)$ is expressed as

$$\hat{\Psi}(\xi)=K_0\xi^2\mathrm{e}^{-\xi^2/2}\chi_{(0,\infty)}(\xi), \tag{7}$$

where $\chi_{(0,\infty)}(\xi)$ denotes the Heaviside step function, which is equal to 1 when $\xi>0$ and equal to 0 otherwise. K_0 denotes a normalization constant.

Let $\psi(x)=\psi^{\mathrm{r}}(x)+\mathrm{j}\psi^{\mathrm{i}}(x)$, whose real part is shown as Eq.(5). By Eq.(6), we obtain the imaginary part:

$$\psi^{\mathrm{i}}(x)=-\frac{1}{\pi}\int_{-\infty}^{+\infty}\frac{\sigma^2}{x-t}\frac{\mathrm{d}^2\theta_\sigma}{\mathrm{d}t^2}\mathrm{d}x. \tag{8}$$

By Eq.(8), the following equation can be inferred:

$$\psi^{\mathrm{i}}(x)=\frac{1}{\pi}\left[\sqrt{2\pi}x-\theta_\sigma'''(x)+2\theta_\sigma'(x)\right]. \tag{9}$$

Then the complex wavelet transform of $f(x)$ is

$$\begin{aligned}Wf^{\mathrm{c}}&=f*\psi_\sigma(x)=\sigma^2 f(x)*\theta_\sigma''(x)+\\&\mathrm{j}\frac{-1}{\pi}\left\{f*\left[\sigma^3\theta_\sigma'''(x)+2\sigma\theta_\sigma'(x)-\sqrt{2\pi}\frac{x}{\sigma^2})\right]\right\}.\end{aligned} \tag{10}$$

Suppose $\mathrm{Re}(f*\psi_\sigma(x))$ is the real part of Wf^{c} and $\mathrm{Im}(f*\psi_\sigma(x))$ is the imaginary part. The wavelet transform modulus maxima can be found by

$$\begin{aligned}\mathrm{d}\,|Wf^{\mathrm{c}}|^2/\mathrm{d}x=2[&\mathrm{Re}(Wf^{\mathrm{c}})\mathrm{Re}((Wf^{\mathrm{c}})')+\\&\mathrm{Im}(Wf^{\mathrm{c}})\mathrm{Im}((Wf^{\mathrm{c}})')]=0.\end{aligned} \tag{11}$$

The corners of the pulse signal correspond to these modulus maxima. Fig.2 shows a sample of pulse signal and corresponding real-valued and complex-valued wavelet transforms computed according to Eq.(5) and Eq.(10), respectively.

The parameters h_{sp}, h_{ef}, h_{fg}, h_{ff}, h_{ee} can be computed based on the corners directly. The parameter C_1 can be extracted by computing the distance between two adjacent modulus maxima. Suppose PSS_1 is the close region when the two points S and S_1 (Fig.1) are jointed by a beeline, then the parameter A_1 is the amount of pixels included in PSS_1, which can be expressed by

$$A_1=\sum_{(x,y)\in PSS_1}1. \tag{12}$$

EXPERIMENTS AND RESULTS

Our experiments will verify three objectives: (1) The proposed approach can detect the characteristics of the pulse signals accurately; (2) The proposed approach is not influenced by the scale s or modulus threshold t, so it is not necessary any more to decide these two parameters, which is a bottleneck in signal processing; (3) The performance of the proposed method is superior to the conventional techniques based on real-valued wavelet transform in the corner detection of pulse signal.

In order to testify the three objectives, several pulse signal samples gathered in clinic were employed in our experiments.

Fig.3 and Fig.4 show two characteristic detection examples using the proposed approach. Fig.3a is an original pulse signal sample without reducing background noise. Fig.3b shows the result obtained by our method. Firstly, the background noise is eliminated by selecting Mexican hat wavelet as the filter and setting scale to 4. Secondly, the features are extracted, shown by "*". Fig.3c is an intercept of Fig.3b, which is approximately one periodic time. We

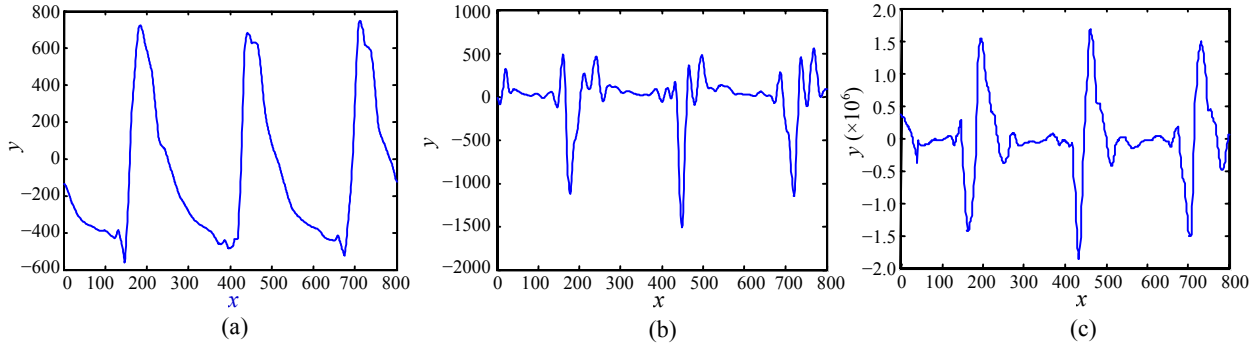

Fig.2 A pulse signal sample and the corresponding wavelet transform
(a) Pulse signal sample; (b) Real-valued wavelet; (c) The wavelet expressed in Eq.(10)

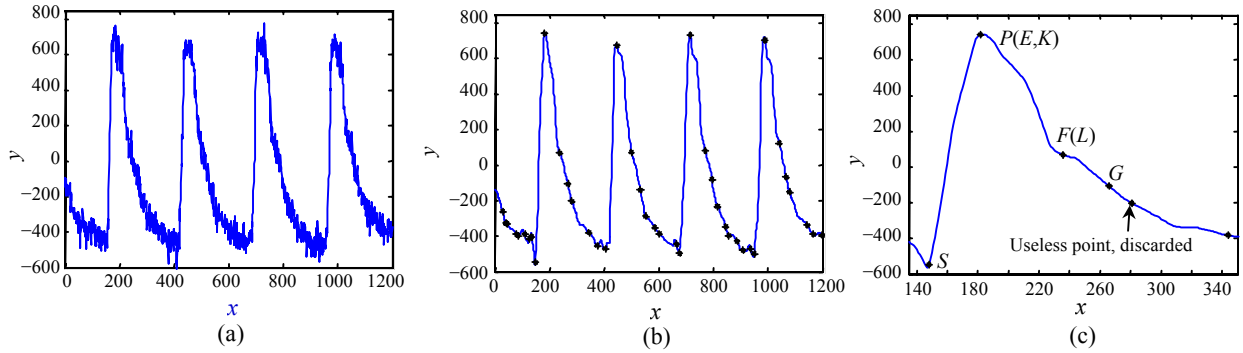

Fig.3 Characteristic detection results based on the proposed method—Example 1
(a) The original pulse signal; (b) Corner detection result; (c) Characteristics label

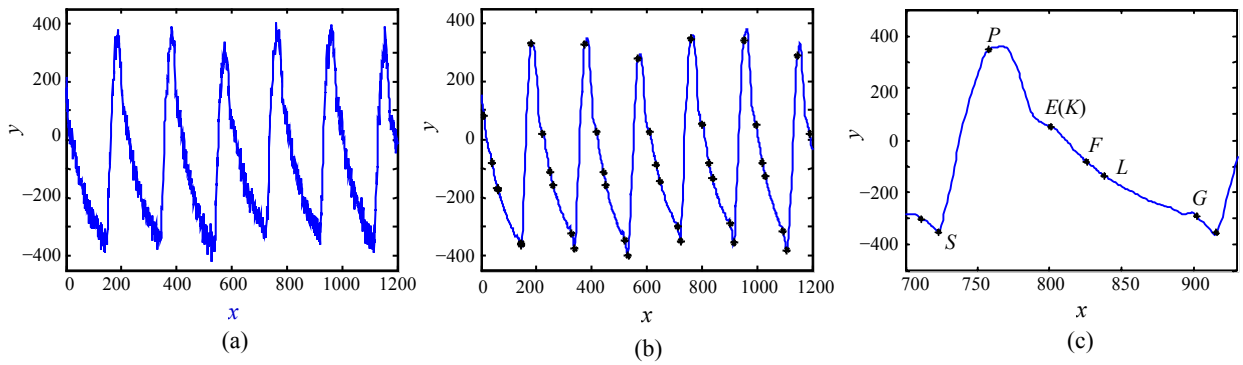

Fig.4 Characteristic detection results based on the proposed method—Example 2
(a) The original pulse signal; (b) Corner detection result; (c) Characteristics label

label these features in Fig.3c by the same letters as those shown in Fig.1. The points P, E, K and the points F, L in Fig.3c are respectively overlapping, which is common in clinic (Fei, 2003).

Fig.4 can be explained in alike manner. From this experiment, it can be seen that the background noises are eliminated effectively and the seven characteristics are located exactly, which validates the first objective.

The influence of modulus threshold t on the detection results is depicted in Fig.5. In addition, to further evaluate the validity of our algorithm, we draw a comparison between the real-valued wavelet and the proposed method. In this experiment, the scale is set to 0.5, at which most characteristics can be detected.

In Figs.5a~5c, we detect the same characteristics, which demonstrate that the modulus threshold t has no influence on the corner detection in our method. Fig.5d gives the detection result based on real-valued wavelet when t=0. It shows that the corners detected are too many to be labelled. The reason is that the modulus of real-valued wavelet is oscillatory (Mallat and Hwang, 1992). To confine the number of the detection corners, t should be set higher. When t=10, the corners are still much more than 7, as shown in Fig.5e. As illustrated in Fig.5f, while t=20, the number of corners is near to 7, but the position is located incorrectly. This experiment testifies that the proposed algorithm outperforms the conventional real-valued wavelet based method in the characteristic detection of pulse signals.

To explore the influence of scale s on the detection results, we design another experiment. We set s to different values and compare the results detected by our method with the conventional real-valued wavelet. The results are shown in Fig.6, which indicates that s has no influence on the corner detection in our algorithm. For real-valued wavelet, Fig.6c shows that when s=0.5, the corners detected are excessive and it is difficult to decide which ones are useful; when s=1.5, the number of the corners is near to that in Fig.6a, but the corners are not the characteristics that we needed. This experiment further validates the second and third objectives.

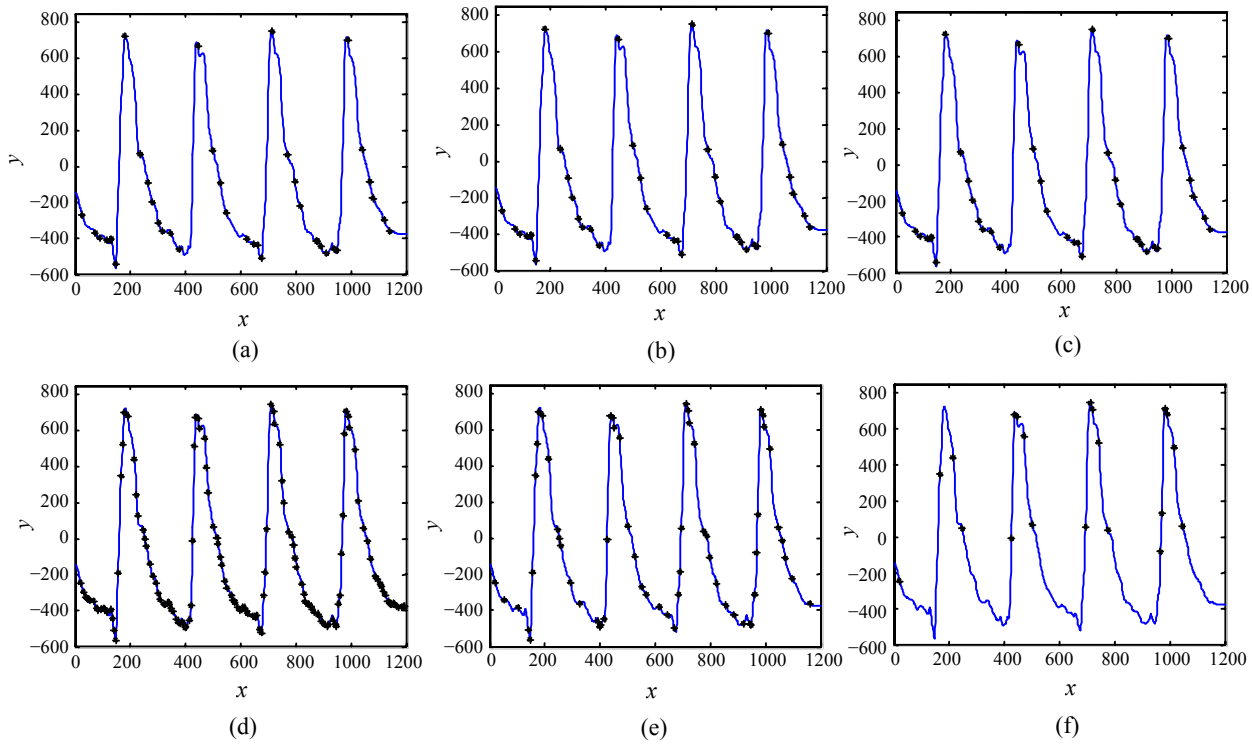

Fig.5 The comparison of characteristic detection results based on real-valued wavelet and the proposed method under different modulus thresholds when the scale is equal to 0.5. *: Characteristic points. (a) Proposed method, t=0; (b) Proposed method, t=10; (c) Proposed method, t=20; (d) Real-valued wavelet, t=0; (e) Real-valued wavelet, t=10; (f) Real-valued wavelet, t=20

The following experiment is constructed for illustrating the advantages of the proposed method over real-valued wavelet method in more detail. We set s=1.5 and t=10, at which the real-valued wavelet method can achieve the best detection result. Fig.7 shows a periodicity of two representative pulse signal samples. The former is a double-humped pulse signal and the latter is a triple-humped pulse signal. It can be seen that the seven characteristic points shown in Fig.1 are all detected and labelled accurately based on the proposed method, as shown in Figs.7a and 7c. In Fig.7b, the characteristic points P, E and K are not detected. In Fig.7c, the characteristic points S, K are missed and P, L depart from their accurate positions.

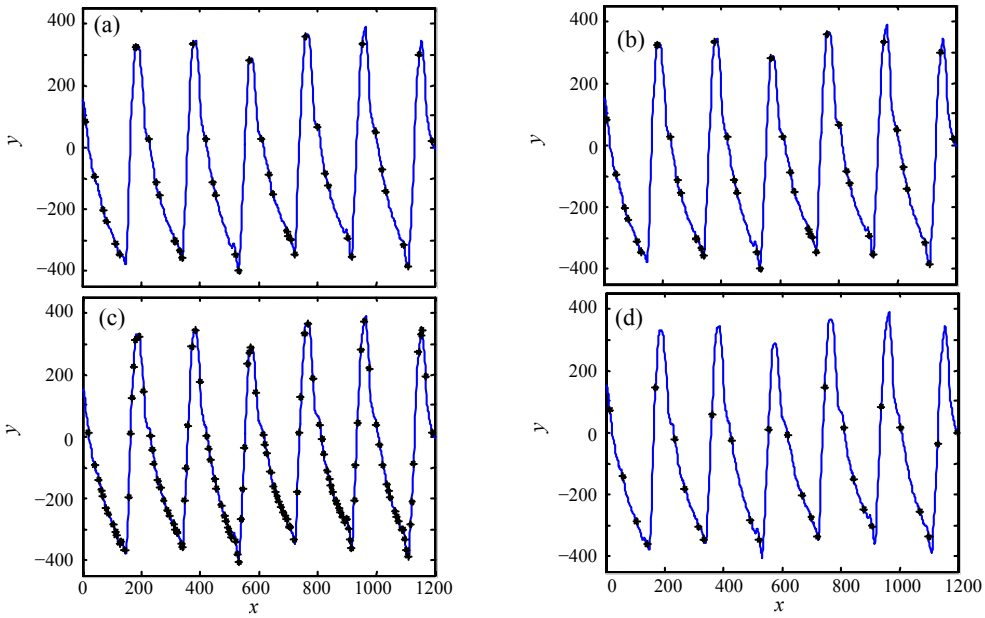

Fig.6 The comparison of characteristic detection results based on real-valued wavelet and the proposed method at different scales when the modulus threshold is equal to zero. *: Characteristic points. (a) Proposed method, s=0.5; (b) Proposed method, s=1.5; (c) Real-valued wavelet, s=0.5; (d) Real-valued wavelet, s=1.5

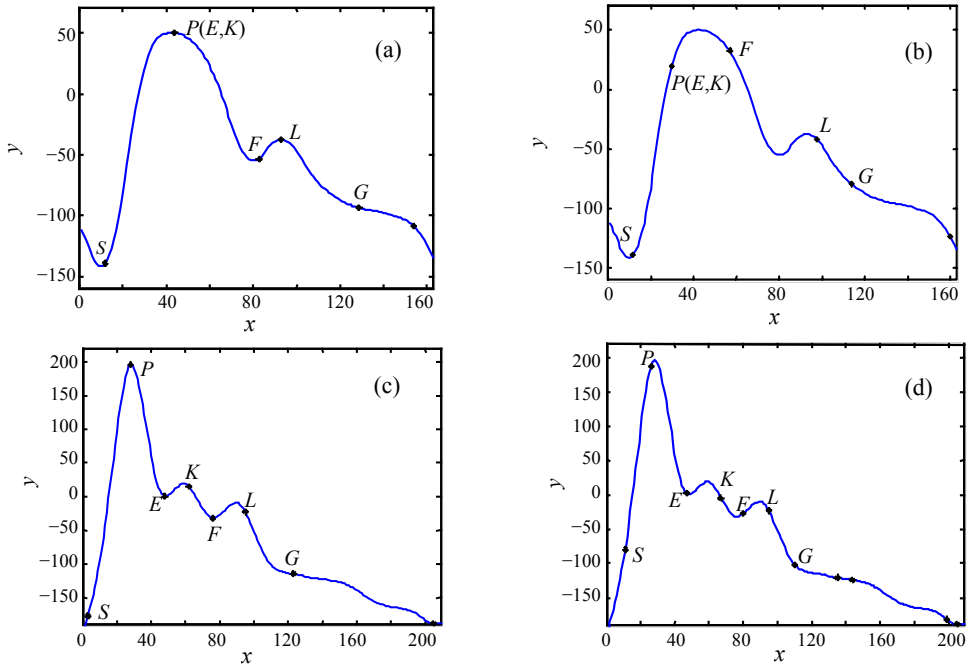

Fig.7 The comparison of detecting and labelling of characteristic points of two pulse signal samples based on real-valued wavelet and the proposed method when s=1.5. *: Characteristic points. (a), (b) are corresponding to one sample and (c), (d) to the other. (a), (c) are results of the proposed method; (b), (d) are results of the real-valued wavelet

CONCLUSION

In this paper, we present a method to realize the extraction of the pulse signal parameters automatically. The proposed method can eliminate the background noises effectively and detect the characteristics of pulse signals accurately. In addition, our method is not influenced by the modulus threshold or the scale, which makes it more convenient to use.

Further work is needed to extend the findings to extract more representative features of pulse signal, which could be very helpful for pulse classification and expected to facilitate popular applications of pulse diagnosis.

ACKNOWLEDGEMENT

We sincerely thank the Pharmaceutical Informatics Institute of Zhejiang University for supplying the pulse signal samples. The authors also thank Prof. Zhang Bo-Li and Dr. Wang Yang with Tianjin University of Traditional Chinese Medicine, for their constructive suggestions and helpful discussions.

References

Fei, Z.F., 2003. Contemporary Sphygmology in Traditional Chinese Medicine. People's Medical Publishing House, Beijing, p.58-73 (in Chinese).

Lee, H.L., Suzuki, S., Adachi, Y., Umeno, M., Shan, K., 1993. Fuzzy Theory in Traditional Chinese Pulse Diagnosis. Proc. Int. Joint Conf. on Neural Networks. Nagoya, Japan, **10**:774-778.

Lee, J.S., Sun, Y.N., Cen, C.H., 1995. Multiscale corner detection by using wavelet transform. *IEEE Trans. on Image Processing*, **4**(1):100-104. [doi:10.1109/83.350810]

Mallat, S., Hwang, W.L., 1992. Singularity detection and processing with wavelet. *IEEE Trans. on Inf. Theory*, **38**(2):617-643. [doi:10.1109/18.119727]

Mallat, S., Zhong, S., 1992. Characterization of signals from multiscale edges. *IEEE Trans. on Pattern Anal. Machine Intell.*, **14**(7):710-732. [doi:10.1109/34.142909]

Quddus, A., Fahmy, M.M., 1999. An Improved Wavelet-based Corner Detection Technique. Proc. IEEE Int. Conf. on Acoustics, Speech, and Signal Processing, **6**:3213-3216.

Sun, L.U., Tang, Y.Y., You, X.G., 2004. Corner Detection for Object Recognition by Using Wavelet Transform. Proc. 3rd Int. Conf. on Machine Learning and Cybernetics. Shanghai, p.26-29.

Tu, C.L., Hwang, W.L., 2005. Analysis of singularities from modulus maxima of complex wavelets. *IEEE Trans. on Inf. Theory*, **51**:1049-1062. [doi:10.1109/TIT.2004.842706]

Wang, H.Y., Cheng, Y.Y., 2005. A Quantitative Model for Pulse Diagnosis in Traditional Chinese Medicine. 27th Annual Int. Conf. of the IEEE Engineering in Medicine and Biology Society. Shanghai, China, p.5676-5679.

Xu, L.S., Zhang, D., Wang, K.Q., Wang, L., 2006. Arrhythmic pulses detection using Lempel-Ziv complexity analysis. *EURASIP J. Appl. Signal Processing*, p.1-12. [doi:10.1155/ASP/2006/18268]

Xu, L.S., Zhang, D., 2007. Baseline wander correction in pulse waveform using wavelet-based cascaded adaptive filter. *Computers Biol. Med.*, **37**(5):716-731. [doi:10.1016/j.compbiomed.2006.06.014]

Yoon, Y.Z., Lee, M.H., Soh, K.S., 2000. Pulse type classification by varying contact pressure. *IEEE Eng. Med. Biol. Mag.*, **19**:106-110. [doi:10.1109/51.887253]